Fluorescent Probe Studies on the Microstructure of Polystyrene–Poly(vinylpyridine) Diblock Copolymer Film

Kenichi Nakashima† **and Mitchell A. Winnik***

Department of Chemistry and Erindale College, University of Toronto, 80 St. George Street, Toronto, Ontario, Canada M5S 1A1

Kevin H. Dai, Edward J. Kramer, and Junichiro Washiyama‡

Bard Hall, Department of Materials Science and Engineering, Cornell University, Ithaca, New York 14853-1501

Received June 3, 1992; Revised Manuscript Received August 28, 1992

ABSTRACT: Several spectroscopic properties of pyrene and its derivatives dissolved in polymer films were examined to investigate the microstructure of polystyrene–poly(2-vinylpyridine) diblock copolymer. Both the fluorescence vibronic structure (I_1/I_3) and fluorescence lifetimes of several of these probes are quite useful as indicators of the polarity of microdomains in the polymers. This finding was applied to study the microstructure of the diblock copolymer film. The results indicate that PS and PVP chains of the copolymer are not randomly mixed but are phase separated, as expected.

Introduction

Fluorescence techniques have been employed for over two decades to study microheterogeneous media.[1-7] Areas of application range from surfactant micelles to polymer blends. These experiments can be divided into two classes: those involving fluorescent *labels*, i.e., the fluorophore covalently bonded to one of the components; and those involving fluorescent *probes*. In probe experiments one adds a dye to the system which will both selectively seek out one component of the system and also, through its fluorescence, report on its environment. Because labeling experiments commonly require difficult syntheses of labeled components, probe experiments are very attractive.

An interesting feature of fluorescent probe experiments is that almost all such experiments have been limited to water-containing media. Such techniques are widely employed in systems involving micelles,[1,2] lipid and synthetic vesicles,[1,3,4] inverse micelles,[1] microemulsions,[1] and water-soluble polymers bearing hydrophobic substituents.[5] These experiments are successful because it is relatively easy to find dyes that partition selectively into either organic or aqueous environments. It is not so straightforward to find probes that partition selectively into two nonaqueous environments. Selective dye adsorption has been used to study silica gel surfaces.[6] One can take advantage of ion-pairing interactions to study ionomers in organic solvents.[7]

We are interested in the possibility that fluorescent probe techniques can be developed to study phase-separated systems composed of organic polymers. These would include polymer blends and block copolymers. An attractive long-range goal for such research is the determination of the critical micelle concentration (cmc) for block copolymers in polymer matrices, taking advantage of the strong sensitivity of certain dyes to the onset of phase separation.[8,9] In this paper we report our first steps in this direction, examining various derivatives of pyrene as fluorescence probes in polystyrene (PS) and poly(2-vinylpyridine) (PVP) films as well as in films prepared from a PS–PVP diblock copolymer. The structure of these dyes is shown in Figure 1. These dyes have significantly different fluorescence properties in PVP compared to PS. We show how these differences can be analyzed in terms of the partition of the dyes between the PS and PVP phases in the block copolymer films. Pyrene derivatives bearing an OH substituent hydrogen bond to PVP with sufficient tenacity that they are found almost exclusively in the PVP domains of the block copolymer.

Experimental Section

1. Synthesis and Characterization of PS, PVP, and PS–PVP. The synthesis and characterization of the polystyrene–poly(2-vinylpyridine) (PS–PVP) diblock copolymer are briefly summarized below, and the details can be found in refs 10 and 11. Synthesis of the copolymer was performed in a solution of tetrahydrofuran (THF) at ca. −55 °C via anionic polymerization using cumylpotassium as the initiator. Following the reaction, the copolymer was precipitated in a copious quantity of hexane and then dried under a reduced pressure. The molecular weight of the PS block was measured by size exclusion chromatography (SEC) using a precursor removed from the reactor prior to the polymerization of the second block, poly(2-vinylpyridine). The molecular weight of PVP block was determined based on the ratio of repeat monomer units of PVP to PS measured by NMR and the molecular weight of PS precursor measured by SEC. In this way, the molecular weights of the PS and PVP blocks were determined to be 100K and 100K, respectively. In addition, SEC was also utilized to ensure that a narrow molecular weight distribution ($M_w/M_n \approx 1.1$) of the resulting copolymer was achieved. A PVP homopolymer with dispersity ~ 1.2 was synthesized by similar procedures to those described above, and the molecular weight was determined to be 300K by SEC using PS standards as reference. A monodisperse PS homopolymer of molecular weight 670K from Polysciences Inc. was used as received.

2. Probe Molecules. Pyrene (Aldrich) was recrystallized from ethanol; 4-(1-pyrenyl)butanoic acid (Aldrich) was used as received. 1-Pyrenemethanol was prepared by $NaBH_4$ reduction of 1-pyrenecarboxaldehyde (Aldrich); 4-(1-pyrene)butanol was prepared by reduction ($LiAlH_4$) of pyrenebutanoic acid. 1-Pyrenemethyl hexyl ether was prepared by treating pyrenemethanol in dimethylformamide with NaH and subsequently adding an excess of 1-bromohexane. The product (mp = 56 °C) was purified by repeated recrystallization from ethanol. All probes showed only a single spot by thin-layer chromatography.

3. Preparation of Polymer Films. For the fluorescence experiments, a trace amount (approximately 100 ppm) of each

---

* To whom correspondence should be addressed.

† On leave from the Laboratory of Chemistry, College of Liberal Arts, University of Saga, 1 Honjo, Saga 842, Japan.

‡ Present address: Showa Denko K.K., 3-2, Chidori-cho, Kawasaki-ku, Kawasaki 210, Japan.

0024-9297/92/2225-6866$03.00/0

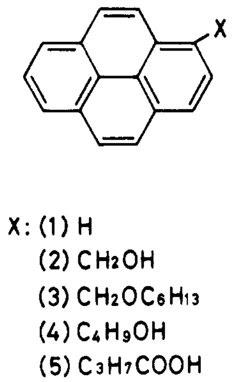

Figure 1. Structures of the probes employed.

Table I
Relative Band Intensities I_1/I_3 of the Fluorescence Spectra of Pyrene and Its Derivatives in Films of PS, PVP, and PS–PVP

	I_1/I_3			
probe	PS	PVP	PS–PVP	R_I (%)
Py-H	1.05	1.49	1.10	29.6
Py-CH_2OH	1.30	1.93	1.83	32.9
Py-$CH_2OC_6H_{13}$	1.08	1.40	1.15	22.8
Py-C_4H_9OH	3.17	3.49	3.48	9.2
Py-C_3H_7COOH	2.73	3.47	3.43	21.3

different fluorescence probe was added to a solution of one of the polymers (PS, PVP, PS–PVP) in THF. These polymer solutions were then used to cast films on glass slides for the fluorescence measurements. The resulting films of thickness ~2 μm were dried in air over a 48-h period before fluorescence measurements were made.

For transmission electron microscopic observation, a film of the diblock copolymer with a thickness around 300 Å was cast on a NaCl crystal. The film was floated off onto the surface of water and then picked up on a copper grid. Subsequently, the resulting film on the copper grid was dried and then exposed to iodine vapor at room temperature for 3 h to stain the PVP phase.[25]

4. Measurements. Fluorescence and fluorescence excitation spectra were recorded on a Spex Fluorolog 2 spectrofluorometer or a Hitachi F-4000 spectrofluorometer, with front-face configuration for detection. The excitation wavelength for fluorescence spectra and emission wavelength for monitoring excitation spectra were 335 and 400 nm, respectively, if not stated otherwise. Both fluorescence and excitation spectra were corrected by a conventional method with rhodamine B.

Fluorescence decay curves were measured with the picosecond single-photon-timing technique. The samples were excited by a synchronously pumped, cavity dumped dye laser (Coherent 701-3) equipped with a second-harmonic generator. The laser dyes employed were rhodamine 6G or DCM. The fluorescence emission was detected by a microchannel-plate detector (Hamamatsu R1564U-01). The pulse width (fwhm) of an instrumental response function of the scattered laser light was 100 ps. The decay curves were analyzed by using an iterative nonlinear least-squares deconvolution program.

Results and Discussion

1. Vibronic Fine Structure of the Fluorescence from the Probes in Polymers. Fluorescence spectra of pyrene in PS, PVP, and PS–PVP are shown in Figure 2. The assignment of each band has been well established.[8,9] Band I is the origin band of the $S_1 \rightarrow S_0$ transition. As $S_1(B_{3u}^-) \rightleftarrows S_0(A_g^-)$ transitions are forbidden due to the selection rule on the configuration interaction for *even alternant* hydrocarbons with D_{2h} symmetry,[12] the origin band can be only very weakly observed in the vapor phase.[13] The relatively strong appearance of the origin band in condensed phases is due to the perturbation by solvents. The intensity of the origin band increases with increasing polarity of the solvent (or environment). Alternatively, the intensity of band III is almost independent of the solvents. The band has been assigned as a b_{1g} vibration. It has been shown that forbidden vibronic bands in forbidden electronic transitions of a wide variety of organic molecules show marked intensity enhancement by the solvent perturbation.[14-17] This effect is especially conspicuous in the case of pyrene. Since the intensity of band I is quite sensitive to the polarity of the solvent compared to that of band III, the intensity ratio of the two bands, which is denoted by I_1/I_3, has been widely used for probing the structures of microheterogeneous systems such as micelles, vesicles, Langmuir–Blodgett films, and polyelectrolytes,[1] although there remain some unresolved issues about the origin of the solvent intensification effect.[9,18-21]

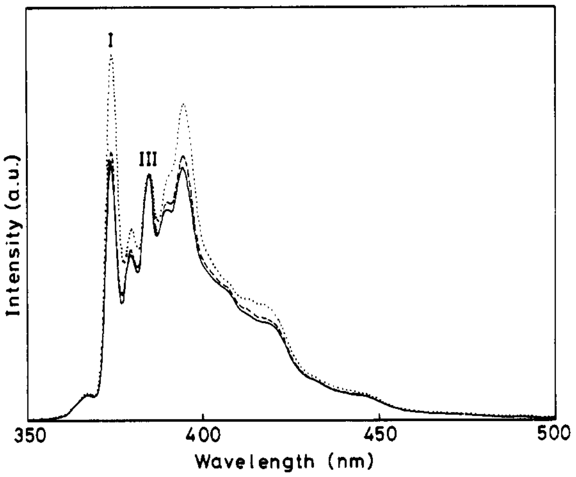

Figure 2. Fluorescence spectra of pyrene in the films of PS (—), PVP (···), and PS–PVP (- - -). The spectra are normalized for convenience at band III.

Here we use the intensity ratio I_1/I_3, to examine the microstructure of PS–PVP films. Table I summarizes the I_1/I_3 values for the five probes in PS, PVP, and PS–PVP films. Pyrene, 1-pyrenemethanol, 1-pyrenemethyl hexyl ether, and 1-pyrenebutanoic acid show a drastic change of I_1/I_3 values on going from PS to PVP, whereas 1-pyrenebutanol does not. For the present study the probe should satisfy two conditions: (i) it shows a significant change of the spectroscopic signal on going from PS to PVP matrices and (ii) the partition of the probe between PS and PVP phases is strongly biased to one phase. To discuss point i quantitatively we define the extent of the change of the I_1/I_3 value, R_I, by

$$R_I = 100[(I_1/I_3)_{PVP} - (I_1/I_3)_{PS}]/(I_1/I_3)_{PVP} \qquad (1)$$

The larger the R_I value, the better the probe. Thus we can see that 1-pyrenebutanol is an inferior probe to the others from the viewpoint of i. As for item ii, we can assess the suitability of each probe by comparing its I_1/I_3 value in PS–PVP with that in PS and PVP. It is notable that pyrene and 1-pyrenemethyl hexyl ether show similar I_1/I_3 values between PS–PVP and PS films, while 1-pyrenemethanol, 1-pyrenebutanol, and 1-pyrenebutanoic acid show similar I_1/I_3 values between PS–PVP and PVP films. These results indicate that pyrene and 1-pyrenemethyl hexyl ether are preferentially solubilized in the PS phase of the PS–PVP film, while 1-pyrenemethanol, 1-pyrenebutanol, and 1-pyrenebutanoic acid are segregated into the PVP phase of the PS–PVP film. In conclusion, the probes, except for 1-pyrenebutanol, satisfy both of the two conditions and thus can be considered as candidates of the probes for the present study.

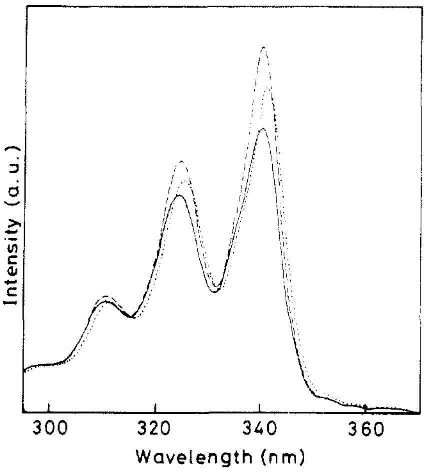

Figure 3. $S_2 \leftarrow S_0$ fluorescence excitation spectra of pyrene in the films of PS (—), PVP (···), and PS–PVP (- - -).

Table II
Location of the Origin Bands for $S_2 \leftarrow S_0$ Transitions of Pyrene and Its Derivatives in Films of PS, PVP, and PS–PVP

	wavelength (nm)		
probe	PS	PVP	PS–PVP
Py-H	341.5	342.0	341.5
Py-CH_2OH	348.5	349.5	349.5
Py-$CH_2OC_6H_{13}$	347.5	348.0	347.5
Py-C_4H_9OH	349.0	350.0	350.0
Py-C_3H_7COOH	349.0	348.0	349.0

2. Band Shift of the $S_2 \leftarrow S_0$ Transition Due to the Effect of Polymer Matrices. Figure 3 shows the $S_2 \leftarrow S_0$ fluorescence excitation spectra of pyrene in PS, PVP, and PS–PVP polymer films. Since the films are not thick enough to allow us to observe directly the $S_2 \leftarrow S_0$ absorption, we observed the $S_2 \leftarrow S_0$ excitation spectra instead. The resemblance of the excitation spectra in PS or PVP to the $S_2 \leftarrow S_0$ absorption spectra in toluene or pyridine supports our claim that either spectrum gives us the same basic information. In Table II are listed the positions of the origin bands for the $S_2 \leftarrow S_0$ transitions of pyrene and its family in the polymers. The band positions for pyrene and 1-pyrenemethyl hexyl ether in PS–PVP film are the same as those in PS film, whereas the positions for the rest of the probes in PS–PVP film are the same as those in PVP film. This suggests that pyrene and 1-pyrenemethyl hexyl ether are located in the PS phase of the PS–PVP film and the remaining derivatives are concentrated in the PVP phase. However, the spectral shifts are quite small for all the probes on going from PS to PVP films and thus not suitable for quantitative analysis of dye partitioning between the phases.

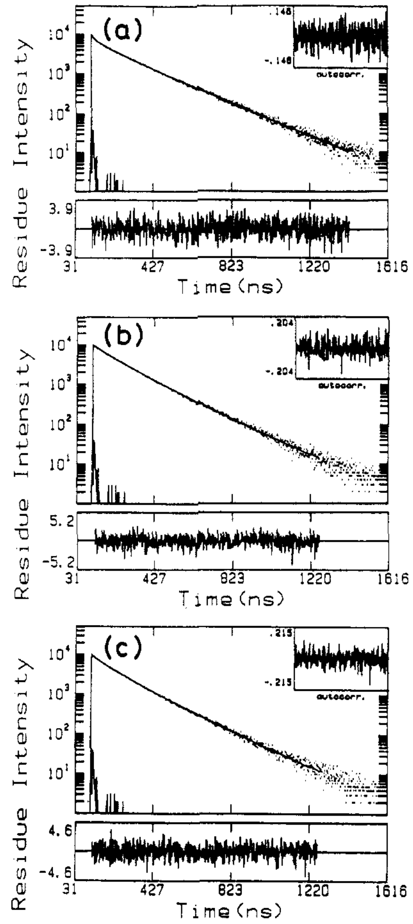

Figure 4. Fluorescence decay curves of 1-pyrenemethanol in the films of PS (a), PVP (b), and PS–PVP (c).

Table III
Fluorescence Lifetimes of Pyrene and Its Derivatives in Films of PS, PVP, and PS–PVP

	mean lifetime (ns)			
probe	PS	PVP	PS–PVP	R_T (%)
Py-H	278	235	262	18.5
Py-CH_2OH	187	162	160	15.3
Py-$CH_2OC_6H_{13}$	205	185	200	10.6
Py-C_4H_9OH	155	130	131	19.2
Py-C_3H_7COOH	167	139	143	19.8

3. Fluorescence Lifetimes of the Probes in Polymers. Representative fluorescence decay curves are shown in Figures 4. The decay curves do not show a single-exponential profile even in the case of the pure PS or PVP homopolymer. The nonexponential decay may be attributed to the presence of a distribution of sites for probe molecules in the polymer environment. Since the probe may have a different lifetime in each site, we could, in principle, analyze the decay curve with a series of exponentials whose number is the same as the number of the sites or by means of some appropriate distribution function. Here we are not so much interested in the details of how the probe is solubilized in each polymer as we are with the much larger decay rate differences of the probe in PS vs PVP environments. Therefore, we use a sum of three exponentials as a convenient way of parameterizing the $I(t)$ decay profile. We do not ascribe theoretical significance to the individual decay parameters but rather use these parameters to calculate mean decay times $\langle\tau\rangle$ from the data.

$$\langle\tau\rangle = \sum_i A_i\tau_i^2 / \sum_i A_i\tau_i \qquad (2)$$

where A_i and τ_i denote the preexponential factor and the lifetime of the ith component (i = 1–3). The results are presented in Table III. All of the probes seem to show a significant change in lifetime on going from PS to PVP films. For the sake of quantitative discussion, we define the extent of change of lifetime, R_T, by an equation similar to eq 2:

$$R_T = 100[\langle\tau\rangle_{PS} - \langle\tau\rangle_{PVP}]/\langle\tau\rangle_{PVP} \qquad (3)$$

R_T values obtained are presented in Table III, ranging from 10 to 20%. These values seem to be large enough to make the mean lifetime a useful probe of the structure of the polymers.

All probes show a decrease in mean lifetime as they are transferred from PS to PVP films. Part of this decrease can be explained by a solvent effect on the $S_1 \rightarrow S_0$

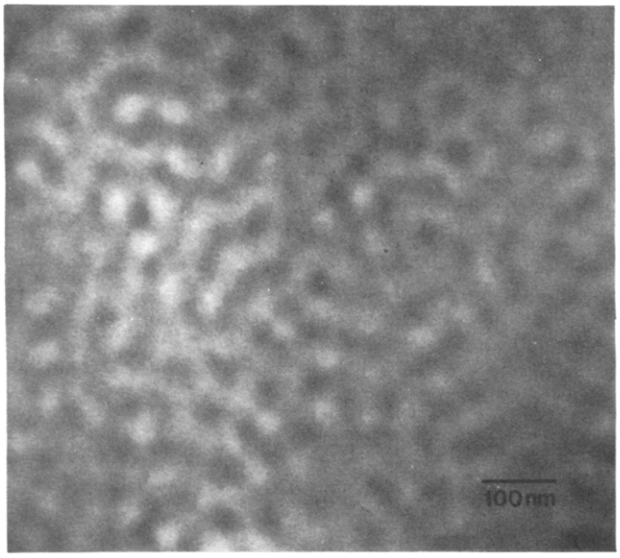

Figure 5. TEM micrograph of an as-cast film of the diblock copolymer stained with iodine (dark phase, PVP phase; bright phase, PS phase).

transition of pyrene. As we stated, the $S_1 \rightarrow S_0$ transition of pyrene is forbidden due to its high symmetry. When this molecule is surrounded by solvent molecules, its molecular orbitals will be distorted by the effect of the field from its surroundings. The distortion of molecular orbitals makes the $S_1 \rightarrow S_0$ transition slightly allowed, resulting in an increment of both the radiative decay rate (i.e., the decrease of lifetime) and the intensity of the origin band. Generally, the more polar solvent causes the larger deformation of molecular orbitals of pyrene. Therefore, the lifetime of pyrene is shorter in PVP than in PS matrices. The same explanation can be given to the pyrene derivatives.

Distortion of molecular orbitals will also be caused by introducing substituents onto pyrene, explaining why the lifetimes of the substituted pyrenes are shorter than that of pyrene itself. The lifetime shift from pyrene is largest in 1-pyrenebutanol (see Table III). When the electronic transition becomes more allowed, the intensity of the origin band becomes less affected by solvents. It is for this reason that the I_1/I_3 ratio of 1-pyrenebutanol is insensitive to the polarity of the polymer environment in which it is dissolved (see Table I).

An additional effect, which may in fact be dominant here, is the role of the matrix in promoting radiationless deactivation of the S_1 state of pyrene. This weak quenching can occur through charge transfer interactions with the medium. One can distinguish quenching effects from symmetry effects through careful quantum yield measurements.

4. Formation of the Associated Structures of PS and PVP Chains in the Film of PS–PVP Diblock Copolymer. PS and PVP are highly immiscible polymers, characterized by a value of $\chi \approx 0.1$.[10,22] For the polymer examined here, $\chi N \approx 200$, where $N \approx 2000$ is the total degree of polymerization of the block copolymer. This implies a strong driving force for the block copolymers in bulk to undergo microphase separation. This view is confirmed by transmission electron microscopy (Figure 5), where we see domains of PVP selectively stained by iodine. The fluorescence probes also indicate that segregated microphases exist in the system. This information is most evident from those probes bearing OH group substituents. For example, the I_1/I_3 ratios of 1-pyrenebutanol and 1-pyrenebutanoic acid in the PS–PVP films are very close to those in PVP itself. The lifetimes of 1-pyrenemethanol and 1-pyrenebutanol in PS–PVP show the same trend. We anticipate hydrogen bonding between the OH group and a pyridine unit. The probe parameters indicate that these pyridine units are located in domains strongly resembling pure PVP.

Table IV
Calculated Partition Coefficients of Pyrene and Its Derivatives between the PS and PVP Phases in PS–PVP Diblock Copolymer

	K	
probe	I_1/I_3	lifetime
Py-H	0.148	0.585
Py-CH_2OH	5.17	∞
Py-$CH_2OC_6H_{13}$	0.280	0.333
Py-C_4H_9OH	31.3	24.0
Py-C_3H_7COOH	17.5	5.54

5. Partitioning of the Probes between PS and PVP Microdomains in PS–PVP Diblock Copolymer. Under the condition that the PS and PVP chains in the PS–PVP diblock copolymer are strongly segregated, we can express the measured I_1/I_3 and $\langle\tau\rangle$ values in forms of the amount of probe in each phase of the film.

$$(I_1/I_3)_{BCP} = x(I_1/I_3)_{PVP} + (1-x)(I_1/I_3)_{PS} \tag{4}$$

$$\langle\tau\rangle_{BCP} = x\langle\tau\rangle_{PVP} + (1-x)\langle\tau\rangle_{PS} \tag{5}$$

where x is the molar fraction of the probe in PVP domain. The subscript BCP denotes the diblock copolymer; PS and PVP denote PS and PVP domains in the copolymer, respectively. From eq 4 and 5 we get

$$x = [(I_1/I_3)_{BCP} - (I_1/I_3)_{PS}]/[(I_1/I_3)_{PVP} - (I_1/I_3)_{PS}] \tag{6}$$

$$x = [\langle\tau\rangle_{BCP} - \langle\tau\rangle_{PS}]/[\langle\tau\rangle_{PVP} - \langle\tau\rangle_{PS}] \tag{7}$$

The partition coefficient, K, of the probe between the PS and PVP microphases in the PS–PVP copolymer can be calculated by

$$K = [\text{probe}]_{PVP}/[\text{probe}]_{PS} = xV_{PS}/(1-x)V_{PVP} \tag{8}$$

where V_{PVP} and V_{PS} denote the total volumes of the PVP and PS microphases, respectively. To calculate x and K by eq 6–8 we assumed that $(I_1/I_3)_{PS}$ and $(I_1/I_3)_{PVP}$ or $\langle\tau\rangle_{PS}$ and $\langle\tau\rangle_{PVP}$ have the same values as those in the homopolymer (i.e., the values in Tables I and III). The values of V_{PS} and V_{PVP} were estimated from the molecular weights of the PS and PVP chains in the PS–PVP copolymer and the densities of the respective homopolymers. The results are summarized in Table IV. If we look at 1-pyrenemethyl hexyl ether and 1-pyrenebutanol, we can see that the partition coefficients obtained from the I_1/I_3 values agree well with those obtained from the lifetimes. This agreement assures us of the reliability of the results. In the cases of the other probes, the I_1/I_3 ratios and the lifetimes give somewhat different values of K. However, the partition coefficients obtained from two kinds of spectroscopic parameters show the same tendency for the distribution of the probes in the PS–PVP diblock copolymer: that is, pyrene and 1-pyrenemethyl hexyl ether preferentially reside in the PS phase, whereas 1-pyrenemethanol, 1-pyrenebutanol, and 1-pyrenebutanoic acid preferentially reside in the PVP phase.

Concluding Remarks

It has been shown that fluorescence techniques employing pyrene and its derivatives as fluorescent probes have a significant potential for the study of the microstructure of PS–PVP diblock copolymer films. The advantage of the present technique comes from its high sensitivity as well as the variety of the spectroscopic parameters one can measure. The concentrations of the probes needed for fluorescence techniques are orders of magnitude lower than those for UV or IR absorption spectroscopies. The high sensitivity makes it possible to use probes at such low concentrations that the probe molecules do not perturb the structure of the materials.

The next attempt for us will be to investigate the associating behavior (micelle formation) of PS–PVP diblock copolymers in PS homopolymer matrices. Experiments,[11,22–24] as well as general thermodynamic considerations, suggest that PS–PVP copolymer forms micelles in the PS matrix above a critical micelle concentration. To have a rapid method to detect the critical micelle concentration and to follow the kinetics of micelle formation in the melt are not only scientifically interesting but also very important practically because such information can become the basis for the design of polymer alloys. Such an investigation is now in progress.

Acknowledgment. K.H.D. and E.J.K. acknowledge the support of the Cornell Materials Science Center (MSC) (funded by the NSF–DMR–MRL program) and Dow Chemical through the Polymer Outreach Program of the MSC. M.A.W. and K.N. thank NSERC Canada for their financial support. The authors thank Dr. A. Kats for her synthesis of 4-(1-pyrenyl)methyl hexyl ether and Mr. Jianrong Feng for the sample of 1-pyrenemethanol.

References and Notes

(1) Kalyanasundaram, K. *Photochemistry in Microheterogeneous Systems*; Academic Press, Inc.: New York, 1987.

(2) Zana, R., Ed. *Surfactant Solutions*; Marcel Dekker: New York, 1987.

(3) (a) Wehry, E. L., Ed. *Modern Fluorescence Spectroscopy*; Plenum: New York, 1976; Vols. 1 and 2. (b) Chen, R. F.; Edelhoch, H., Eds. *Biochemical Fluorescence*; Marcel Dekker: New York, 1976; Vols. 1 and 2.

(4) Honda, K., Ed. *Photochemical Processes in Organized Molecular Systems*; North Holland Publ.: Amsterdam, 1991.

(5) (a) Winnik, F. M.; Winnik, M. A.; Ringsdorff, H.; Venzmer, J. *J. Phys. Chem.* **1991**, *95*, 2583. (b) Winnik, F. M.; Winnik, M. A. *Polym. J.* **1990**, *22*, 482. (c) Wilhelm, M.; Zhao, C.-L.; Wang, Y.; Xu, R. L.; Winnik, M. A.; Mura, J. L.; Riess, G.; Croucher, M. D. *Macromolecules* **1991**, *24*, 1033. (d) Strauss, U. P.; Chiao, Y.-C. *Macromolecules* **1986**, *19*, 355.

(6) (a) Kasnansky, R.; Koike, K.; Thomas, J. K. *J. Phys. Chem.* **1990**, *94*, 4521. (b) Levitz, P.; Drake, J. M.; Klafter, J. *J. Chem. Phys.* **1988**, *89*, 5224.

(7) (a) Morawetz, H.; Wang, Y. *Macromolecules* **1988**, *21*, 107. (b) Dowling, K. C.; Thomas, J. K. *Macromolecules* **1991**, *24*, 4123, 4131.

(8) Nakajima, A. *Bull. Chem. Soc. Jpn.* **1971**, *44*, 3272.

(9) Kalyansundaram, K.; Thomas, J. K. *J. Am. Chem. Soc.* **1977**, *99*, 2039.

(10) Shull, K. R. Ph.D. Thesis, Cornell University, 1990.

(11) Shull, K. R.; Kramer, E. J.; Hadziioannou, G.; Tang, W. *Macromolecules* **1990**, *23*, 4780–4787.

(12) (a) Pariser, R. *J. Chem. Phys.* **1956**, *24*, 250. (b) Hoijtink, G. J.; Velthorst, N. H.; Zandstra, P. J. *Mol. Phys.* **1960**, *3*, 533.

(13) Becker, R. S.; Singh, I. S.; Jackson, E. A. *J. Chem. Phys.* **1963**, *38*, 2144.

(14) Koyanagi, M. *J. Mol. Spectrosc.* **1968**, *25*, 273.

(15) Durocher, G.; Sandorfy, C. *J. Mol. Spectrosc.* **1966**, *20*, 410.

(16) Bayliss, N. S.; Wills-Johnson, G. *Spectrochim. Acta, Part A* **1968**, *24*, 563.

(17) (a) Nakashima, K.; Uchida-Kai, K.; Koyanagi, M.; Kanda, Y. *Bull. Chem. Soc. Jpn.* **1982**, *55*, 415. (b) Nakashima, K.; Koyanagi, M. *Bull. Chem. Soc. Jpn.* **1982**, *55*, 3923.

(18) (a) Nakajima, A. *Spectrochim. Acta, Part A* **1974**, *30*, 860. (b) Nakajima, A. *J. Mol. Spectrosc.* **1976**, *61*, 467. (c) Nakajima, A. *J. Lumin.* **1976**, *11*, 429.

(19) (a) Lianos, P.; Georghiou, S. *Photochem. Photobiol.* **1979**, *30*, 355. (b) Lianos, P.; Georghiou, S. *Photochem. Photobiol.* **1979**, *30*, 843.

(20) (a) Dong, D. C.; Winnik, M. A. *Photochem. Photobiol.* **1982**, *35*, 17. (b) Dong, D. C.; Winnik, M. A. *Can. J. Chem.* **1984**, *62*, 2560.

(21) Nakashima, K.; Koyanagi, M. *Photochem. Photobiol.* **1986**, *44*, 169.

(22) Shull, K. R.; Winey, K. I.; Thomas, E. L.; Kramer, E. J. *Macromolecules* **1991**, *24*, 2748–2751.

(23) Dai, K. H.; Kramer, E. J.; Shull, K. R. *Macromolecules* **1992**, *25*, 220–225.

(24) Shull, K. R.; Kramer, E. J. *Macromolecules* **1990**, *23*, 4769–4779.

(25) Aronson, S.; Wilensky, S. B. *J. Polym. Sci., Polym. Chem. Ed.* **1988**, *26*, 125.

Registry No. (PS)(PVP) (block copolymer), 108614-86-4; PVP, 9003-47-8; PS, 9003-53-6; $Br(CH_2)_5CH_3$, 111-25-1; pyrene, 129-00-0; 1-pyrenebutanoic acid, 3443-45-6; 1-pyrenemethanol, 24463-15-8; 4-(1-pyrene)butanol, 67000-89-9; 1-pyrenemethyl hexyl ether, 144156-87-6; 1-pyrenecarboxaldehyde, 3029-19-4.